

2D Correlation Analysis of Spin-Coated Films of Biodegradable P(HB-co-HHx)/PEG Blends

Min Kyung Kim,^a Soo Ryeon Ryu,^a Isao Noda,[†] and Young Mee Jung^{*}

Department of Chemistry, and Institute for Molecular Science and Fusion Technology, Kangwon National University, Chunchon 200-701, Korea. *E-mail: ymjung@kangwon.ac.kr

[†]The Procter & Gamble Company, West Chester, Ohio 45069, USA

Received August 29, 2011, Accepted September 19, 2011

We investigated thermal behavior of spin-coated films of P(HB-co-HHx)/PEG blends by using infrared-reflection absorption (IRRAS) spectroscopy and 2D correlation spectroscopy. Based on 2D IRRAS correlation spectra, we could determine the sequence of spectral intensity changes with increasing temperature that PEG band changes first and then a band for crystalline component of P(HB-co-HHx) changes before a band for amorphous component. The intensities of bands for PEG and amorphous P(HB-co-HHx) were changed greatly as PEG weigh % of P(HB-co-HHx)/PEG blends increased. Transition temperatures of P(HB-co-HHx)/PEG blends were successfully determined by 2D gradient mapping method. The transition temperature of spin-coated films of 98/2 and 90/10 P(HB-co-HHx)/PEG blends and 80/20 P(HB-co-HHx)/PEG blend determined by 2D gradient map are, respectively, about 137.5 and 132.5 °C. Furthermore, P(HB-co-HHx)/PEG blends show an additional transition temperature that have been interpreted in terms of different lamellar thicknesses in spin coated films.

Key Words : P(HB-co-HHx)/PEG blends, Thermal behavior, 2D correlation spectroscopy, 2D gradient mapping method, Transition temperature

Introduction

Poly(hydroxyalkanoate) (PHA) polymers including poly(3-hydroxybutyrate) (PHB) and PHB-based copolymers, such as poly(3-hydroxybutyrate-co-3-hydroxyhexanoate) (P(HB-co-HHx)), are biodegradable and renewable polymers, which have been studied extensively as environment-friendly polymers.¹⁻⁴ The structure and thermal behavior of PHB and P(HB-co-HHx) copolymers have been investigated by X-ray diffraction (XRD), differential scanning calorimetry (DSC), FTIR spectroscopy, and two-dimensional (2D) correlation spectroscopy.⁵⁻¹⁰ Furthermore, phase separation and thermal behavior of blends of PHB with poly(L-lactic acid) (PLLA), PHB with poly(4-vinylphenol) (PVPh), and P(HB-co-HHx) with PLLA have also been intensively studied by using FTIR imaging spectroscopy, XRD, and DSC.¹¹⁻¹³

We have recently investigated the transition temperature and thermal behavior of spin-coated films of P(HB-co-HHx) (HHx = 3.8, 7.2 and 10.0 mol %) copolymers by using principal component analysis-based 2D correlation (PCA2D) spectroscopy and 2D hetero-spectral IR/XPS correlation analysis.¹⁴⁻¹⁶ Generalized 2D correlation spectroscopy is a well-established analytical technique that provides considerable utility and benefit in various spectroscopic studies of polymers.¹⁷⁻¹⁹ To further assist the interpretation of 2D correlation spectra, we have recently proposed a new two-dimensional (2D) data display scheme to determine transi-

tion temperature of polymers.²⁰⁻²² In this scheme, a set of spectra $A(\nu, T)$, where ν is the wavenumber and T is the temperature, are differentiated with respect to T to create a new data set corresponding to the first derivatives of the form dA/dT . This 2D gradient mapping representation that plots the values of the first derivatives of the absorbance with respect to temperature over the space of temperature vs. wavenumber provides a surprisingly simple and direct method for detecting the transition temperatures. The construction of such a plot helps to directly visualize the entirety of complex spectral events occurring during a transition phenomenon. Most importantly, it exploits the selectivity of individual IR bands to allow the observer to easily and quickly draw connections between the macroscopic transition phenomenon and the molecular scale responses. The location of the minima or maxima in a 2D gradient map enables us to identify changes in molecular environment experienced by different chemical moieties associated with the IR absorption at specific wavenumbers which are undergoing the transition process.²⁰⁻²²

P(HB-co-HHx) type of aliphatic polyester are fully miscible with polyethers, like polyethylene glycol (PEG). Because PEG is by itself biodegradable, the study of P(HB-co-HHx)/PEG blend is of great practical interest. Blends of PEG and several aliphatic polyesters have been studied.²³⁻²⁵ The blend of PHB and PEG showed the full miscibility of PHA and PEG.²³ Na *et al.* reported the miscibility of relatively high molecular weight (MW 300,000) PEO and various PHAs.²⁴ Lim *et al.* has reported the miscibility and crystallization behavior of P(HB-co-HHx) blended with

^aThese authors contributed equally to this work.

methoxyPEG.²⁵ However, thermal behavior like crystallization of P(HB-*co*-HHx) in the presence of PEG has not yet been explored much. Furthermore, no work has ever been reported on thin films of P(HB-*co*-HHx)/PEG blends.

In this study, thermal behavior of spin-coated films of 98/2, 90/10, and 80/20 P(HB-*co*-HHx)/PEG blends were characterized by infrared-reflection absorption spectroscopy (IRRAS). To obtain the detailed information about the thermal behavior of these spin-coated films of 98/2, 90/10, and 80/20 P(HB-*co*-HHx)/PEG blends, we applied 2D correlation spectroscopy to IRRAS spectra obtained during the heating process. We also determined the transition temperatures of spin-coated films of 98/2, 90/10, and 80/20 P(HB-*co*-HHx)/PEG blends by using 2D gradient mapping method. Even a simple T_g determination becomes of interest, as PEG is miscible only in the amorphous region of P(HB-*co*-HHx). It will be useful to explore physical aspects of thin films of P(HB-*co*-HHx)/PEG blends by using 2D IR correlation spectroscopy and 2D gradient mapping method.

Experimental Section

Biodegradable P(HB-*co*-HHx) (HHx = 10.0 mol %) copolymer was obtained from the Procter & Gamble Company, Cincinnati, OH. It was dissolved in hot chloroform, and then precipitated in hexane. The same process was repeated again, re-precipitated in methanol, and vacuum-dried at 60 °C. PEG (number-average molecular weight, M_n is 1,500) was purchased from Sigma-Aldrich Co., Ltd., at highest purity available and used as received without further purification.

Blends of P(HB-*co*-HHx) and PEG were prepared by dissolving each component together in hot chloroform. The blending ratios of P(HB-*co*-HHx)/PEG blends were 98/2, 90/10, and 80/20 by weight.

Pt-coated silicon wafers from Siltron Inc. (Korea) were used as the substrates for spin coating. To prepare spin-coated films, about 2 wt % P(HB-*co*-HHx)/PEG blend solutions dissolved in chloroform were spun onto a Pt-coated silicon wafer at 2000 rpm for 60 s. The thickness of spin-coated films of P(HB-*co*-HHx)/PEG blends was about 400 nm.

The infrared-reflection absorption (IRRAS) spectra were measured at a spectral resolution of 4 cm^{-1} with a Thermo

NICOLET 6700 FT-IR spectrometer equipped with a liquid nitrogen-cooled MCT detector. A seagull accessory of Harrick Scientific Product Inc., which includes a heating block attachment, was used for the IRRAS measurement, and an infrared ray was used at an angle of incidence of 79 °C. To ensure a high signal-to-noise ratio, 64 interferograms were co-added for each measurement. The temperature-dependent IRRAS spectra of spin-coated films of P(HB-*co*-HHx)/PEG blends were measured at an increment of 5 °C in the range of 30–150 °C.

Synchronous and asynchronous 2D correlation spectra were obtained by using the same software as at described previously.²⁶

Results and Discussion

The temperature-dependent IRRAS spectra of spin-coated films of 98/2, 90/10, and 80/20 P(HB-*co*-HHx)/PEG blends, obtained during the heating process from 30 to 150 °C, are shown in Figure 1. There are two distinct bands in the C=O stretching region for 98/2, 90/10, and 80/20 P(HB-*co*-HHx)/PEG blends, a crystalline band at 1724 cm^{-1} and an amorphous band at 1755 cm^{-1} . Trends of the spectral changes of C=O stretching region are very similar to each other for the heating process. The intensity of a crystalline band decreases with increasing temperature, while that of an amorphous band increases. Similar trends of the spectral changes of the C-H deformation, the C-O-C stretching mode, and the C-O stretching mode in 1000–1500 cm^{-1} region and the C-H stretching mode in 2800–3050 cm^{-1} region are also observed in each other for the heating process.

To investigate the details of subtle differences in thermal behavior of 98/2, 90/10, and 80/20 P(HB-*co*-HHx)/PEG blends, 2D correlation analysis was applied to temperature-dependent IRRAS spectra of spin-coated films of 98/2, 90/10, and 80/20 P(HB-*co*-HHx)/PEG blends. Figure 2(a), (b) and (c) show, respectively, synchronous 2D correlation spectra in the region of C=O stretching of spin-coated film of 98/2, 90/10, and 80/20 P(HB-*co*-HHx)/PEG blends. Autopower spectrum extracted along the diagonal line in the synchronous 2D correlation spectrum is given on top of each synchronous 2D correlation spectrum. The corresponding asynchronous 2D correlation spectra are shown in Figure 2(d), (e), and (f). In the synchronous 2D correlation spectra

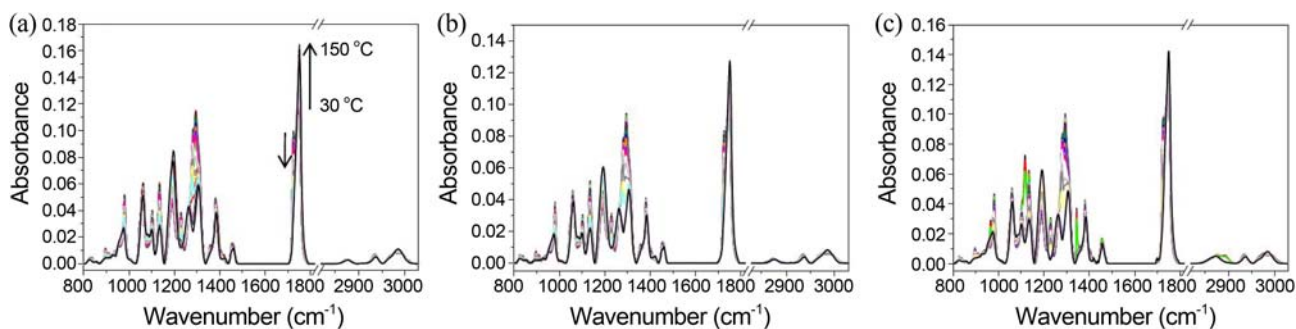


Figure 1. IRRAS spectra of spin-coated films of 98/2 (a), 90/10 (b), and 80/20 (c) P(HB-*co*-HHx)/PEG blends obtained during the heating process from 30 to 150 °C.

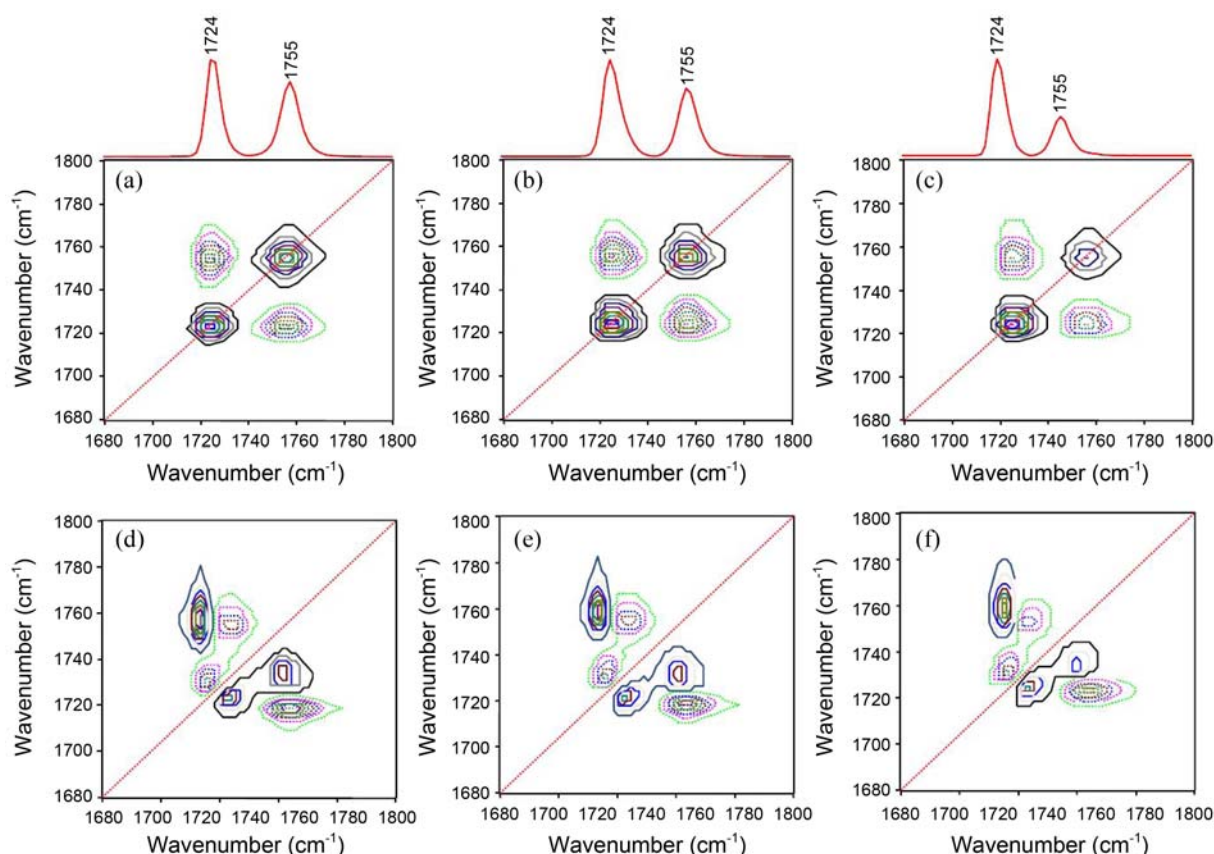


Figure 2. Synchronous (a, b, c) and asynchronous (d, e, f) 2D correlation spectra in the region of C=O stretching mode for spin-coated films of 98/2, 90/10, and 80/20 P(HB-co-HHx)/PEG blends, respectively. The solid and dashed lines represent positive and negative cross peaks, respectively.

in the C=O stretching bands, we can mainly observe the crystalline band at 1724 cm^{-1} and the amorphous band at 1755 cm^{-1} . However, in the asynchronous 2D correlation spectra, the band at 1724 cm^{-1} seems to be resolved into two bands at 1722 and 1729 cm^{-1} , which is not readily detectable in the original 1D spectra. We clearly captured the possible existence of two components in the crystalline band of the C=O stretching mode, i.e., well-ordered primary crystals observed at a lower wavenumber and less ordered secondary crystals observed at a higher wavenumber.¹⁴⁻¹⁶ The sequence of intensity changes in the C=O stretching region with increasing temperature is such that a band of less ordered secondary crystals is changing first and then an amorphous band changes before a band for well ordered primary crystals.

Figure 3(a), (b), and (c) show, respectively, synchronous 2D correlation spectra for the C-H deformation, the C-O-C stretching mode, and the C-O stretching mode in $1000\text{--}1500\text{ cm}^{-1}$ region of spin-coated films of 98/2, 90/10, and 80/20 P(HB-co-HHx)/PEG blends. The corresponding asynchronous 2D correlation spectra are shown in Figure 3(d), (e), and (f). 2D correlation spectra of 80/20 P(HB-co-HHx)/PEG blend are different from those for 98/2 and 90/10 P(HB-co-HHx)/PEG blends. In power spectra extracted along the diagonal line in the synchronous 2D correlation spectra, there are two strongest peaks in 1282 and 1294 cm^{-1} , which

are assigned to amorphous band and crystalline band of P(HB-co-HHx). However, a peak at 1117 cm^{-1} is clearly observed in only 80/20 P(HB-co-HHx)/PEG blends, which can be assigned to PEG. From the analysis of 2D correlation spectra, we can determine the following sequence of spectral intensity changes that PEG band changes first and then a band for crystalline component of P(HB-co-HHx) changes before a band for amorphous component.

Figure 4(a), (b), and (c) show synchronous 2D correlation spectra of spin-coated films of 98/2, 90/10, and 80/20 P(HB-co-HHx)/PEG blends in the region of the C-H stretching in $2800\text{--}3050\text{ cm}^{-1}$. The corresponding asynchronous 2D correlation spectra are shown in Figure 4(d), (e), and (f). 2D correlation spectra of 80/20 P(HB-co-HHx)/PEG blend are different from those for 98/2 and 90/10 P(HB-co-HHx)/PEG blends as expected. For 98/2 and 90/10 P(HB-co-HHx)/PEG blends copolymer, the intensity changes of the bands at 2931 and 2985 cm^{-1} are significant during the heating process, while for 80/20 P(HB-co-HHx)/PEG blends that at 2893 cm^{-1} is great. The intensity of a band at 2893 cm^{-1} is changed greatly as PEG weight % of P(HB-co-HHx)/PEG blends increases, which can be assigned to PEG band. We found that the intensity changes of bands at 2931 and 2985 cm^{-1} for 98/2 and 90/10 P(HB-co-HHx)/PEG blends are more clearly observed than that for 80/20 P(HB-co-HHx)/PEG blends, which can be assigned to P(HB-co-HHx). It

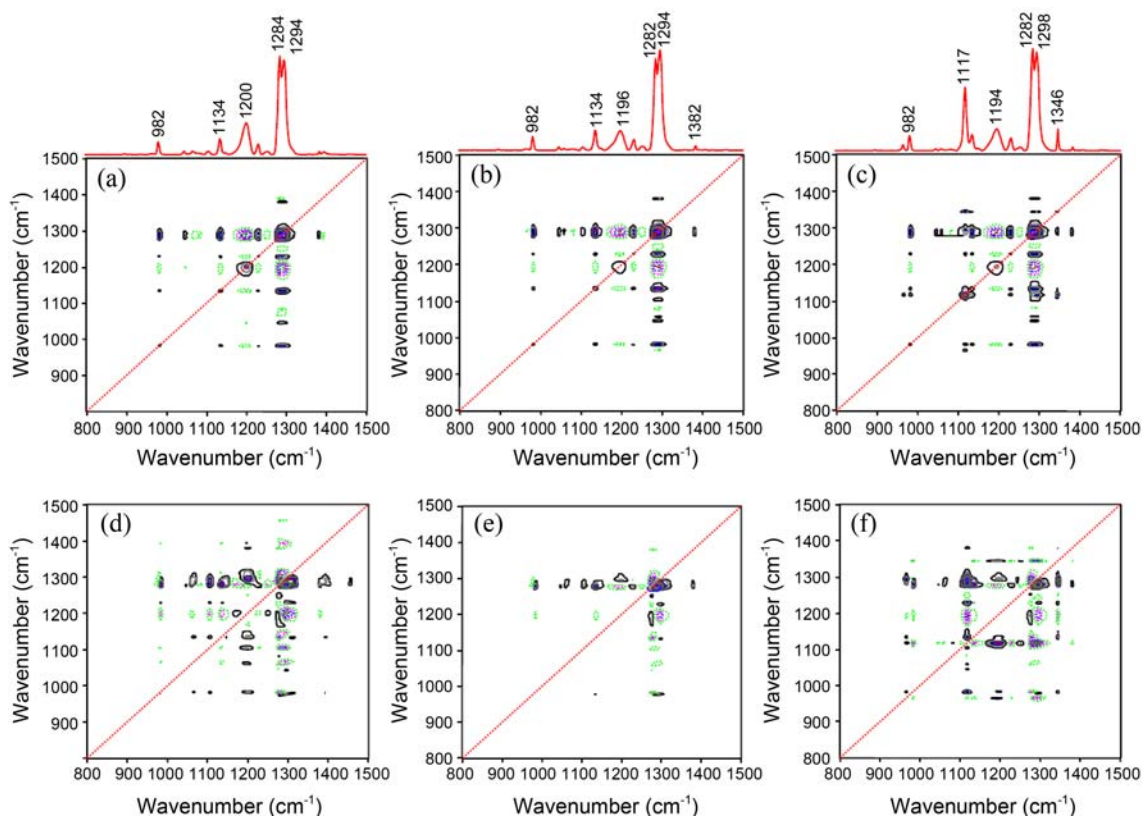


Figure 3. Synchronous (a, b, c) and asynchronous (d, e, f) 2D correlation spectra in the region of C-H deformation, C-O-C stretching, and C-O stretching modes for spin-coated films of 98/2, 90/10, and 80/20 P(HB-co-HHx)/PEG blends, respectively. The solid and dashed lines represent positive and negative cross peaks, respectively.

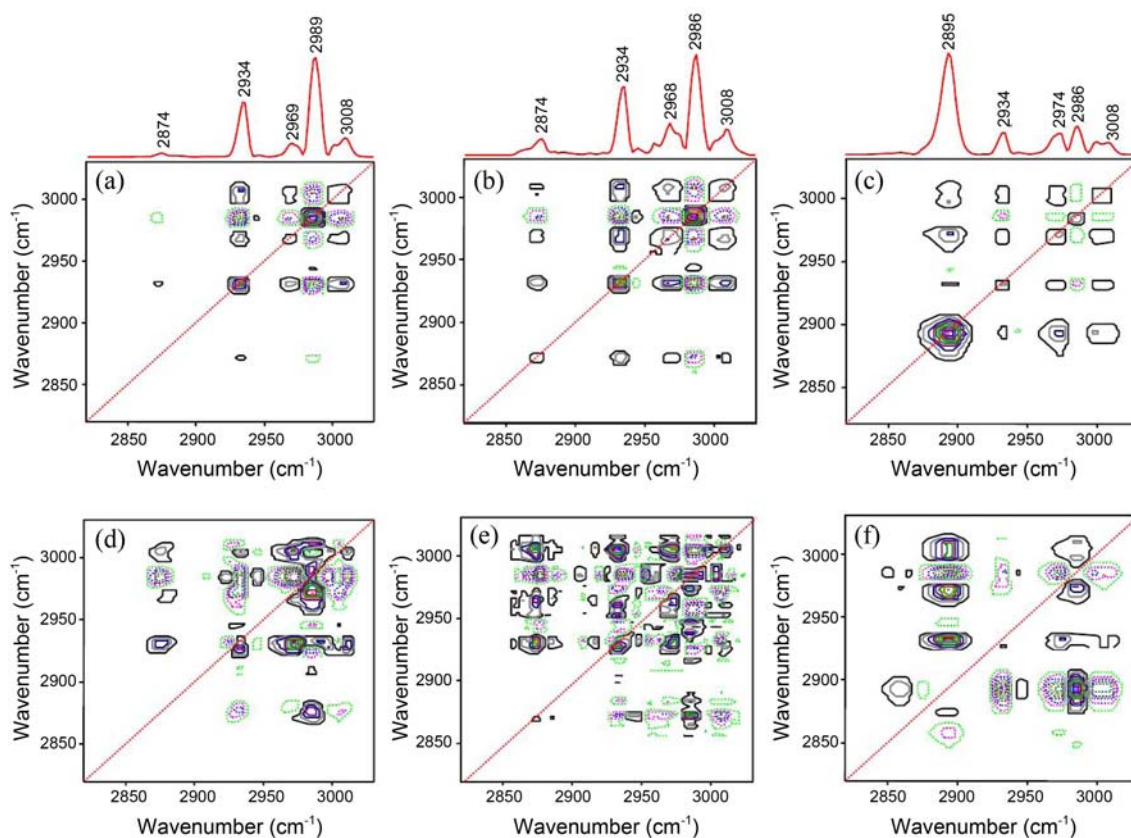


Figure 4. Synchronous (a, b, c) and asynchronous (d, e, f) 2D correlation spectra in the region of C-H stretching mode for spin-coated films of 98/2, 90/10, and 80/20 P(HB-co-HHx)/PEG blends, respectively. The solid and dashed lines represent positive and negative cross peaks, respectively.

Table 1. Band assignments and wavenumber (cm^{-1}) for IRRAS spectra of spin-coated films of P(HB-co-HHx)/PEG blends

2%		10%		20%		Assignments
1D	2D	1D	2D	1D	2D	
981		981		981		CH_2 rocking (PHA C)
1200		1196		1194		C-O-C asymmetric stretching (PHA A)
				1117		C-O-C asymmetric stretching (PEG)
1296	1282	1296	1282	1296	1282	C-O-C asymmetric stretching (PHA A)
	1299		1299		1297	C-O-C asymmetric stretching (PHA C)
				1344		C-O-C asymmetric stretching (PEG)
1724	1722	1724	1722	1724	1722	C=O stretching (well-ordered PHA C)
	1729		1729		1729	C=O stretching (less-ordered PHA C)
1755		1755		1755		C=O stretching (PHA A)
2873		2873		2873		CH_2 asymmetric stretching (PHA C)
				2893		CH_2 asymmetric stretching (PEG C)
2931		2931		2933		CH_2 asymmetric stretching (PHA C)
2972		2974		2974		CH_3 asymmetric stretching (PHA C)
2985		2985		2985		CH_3 asymmetric stretching (PHA A)
3008		3008		3008		Hydrogen bonding

C: crystalline, A: amorphous, PHA: P(HB-co-HHx)

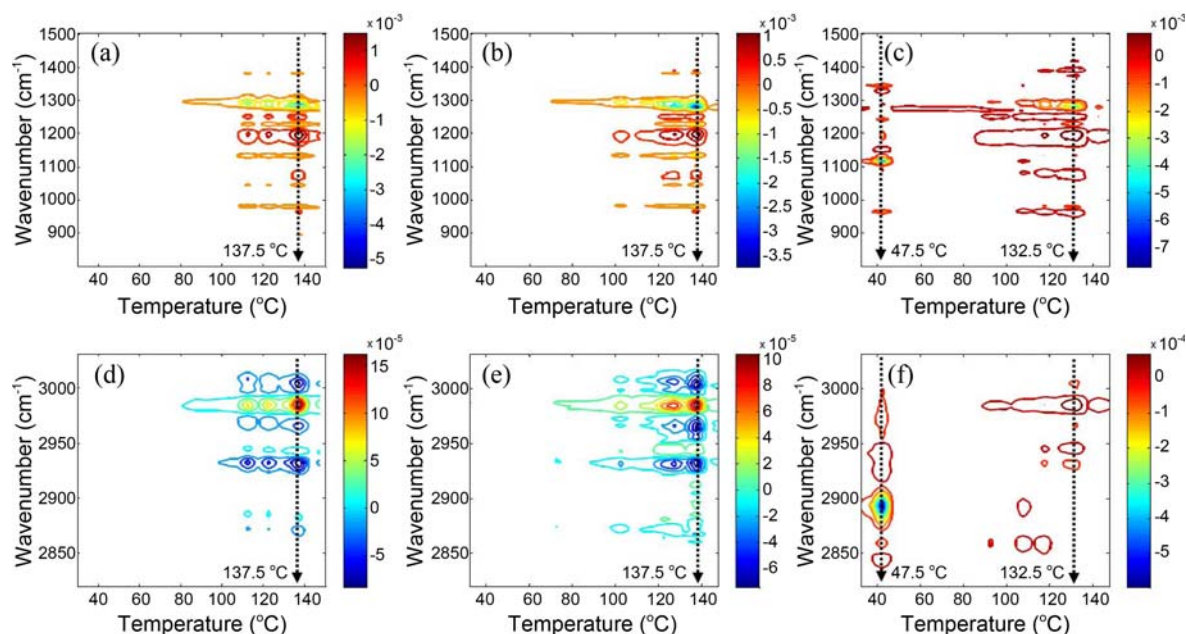


Figure 5. 2D gradient map that plots the values of the first derivatives of the absorbance of IRRAS spectra of spin-coated films of 98/2 (a, d), 90/10 (b, e), and 80/20 (c, f) P(HB-co-HHx)/PEG blends obtained during the heating process with respect to temperature over the space of temperature vs. wavenumber on a single map.

means that the spectral changes of PEG in the C-H stretching region during the heating process are much more significant than those in the C-H deformation, the C-O-C stretching mode, and the C-O stretching regions. Detailed band assignments for IRRAS spectra and 2D correlation spectra of spin-coated films of 98/2, 90/10, and 80/20 P(HB-co-HHx)/PEG blends are summarized in Table 1.

We have previously determined the glass transition temper-

ature of the polymer thin films by using a 2D gradient mapping representation that plots the values of the first derivatives of the absorbance with respect to temperature over the space of temperature vs. wavenumber on a single map.²⁰⁻²² This 2D mapping representation indicates the exact temperature at which the intensities of pertinent bands sensitive to the polymer conformation change most rapidly. Such changes are not always obvious from the conventional

1D FT-IR spectra. Figure 5 gives the gradient 2D maps of dA/dT that plots the values of the first derivatives of the absorbance with respect to temperature over the space of temperature vs. wavenumber. The highest value of dA/dT of spin-coated films of 98/2 and 90/10 P(HB-co-HHx)/PEG blends are observed near 137.5 °C for all bands, while that of 80/20 P(HB-co-HHx)/PEG blend is 132.5 °C. Thus, the transition temperature of spin-coated films of 98/2 and 90/10 P(HB-co-HHx)/PEG blends and 80/20 P(HB-co-HHx)/PEG blend determined by 2D gradient map are, respectively, about 137.5 and 132.5 °C. The transition temperature of spin-coated films of P(HB-co-HHx)/PEG blends decreased as PEG composition of P(HB-co-HHx)/PEG blends increases. It seems that 10 wt % PEG is attributed to more amorphous components. Furthermore, spin coated films of P(HB-co-HHx)/PEG blends show more transition temperature that have been interpreted in terms of different lamellar thicknesses in spin coated films.²⁷ Thermal transition temperature of bulk samples for three different compositions, 98/2, 90/10 and 80/20 P(HB-co-HHx)/PEG blends, measured by DSC-TGA were 128, 121, and 112 °C, respectively. The transition temperatures determined by 2D gradient mapping method in this study reflect the melting of P(HB-co-HHx)/PEG blends.

Conclusion

We demonstrated the thermal behavior of spin-coated films of P(HB-co-HHx)/PEG blends by using 2D IRRAS correlation spectroscopy. From the analysis of 2D correlation spectra, we can determine the following sequence of spectral intensity changes that PEG band changes first and then a band for crystalline component of P(HB-co-HHx) changes before a band for amorphous component. The intensities of bands for PEG and amorphous P(HB-co-HHx) are changed greatly as PEG content of P(HB-co-HHx)/PEG blends increases. The spectral changes of PEG in the C-H stretching region during heating process are much more significant than those in the C-H deformation, the C-O-C stretching mode, and the C-O stretching regions.

Transition temperature of spin coated films of P(HB-co-HHx)/PEG blends were determined by 2D gradient mapping method. The transition temperature of spin-coated films of 98/2 and 90/10 P(HB-co-HHx)/PEG blends and 80/20 P(HB-co-HHx)/PEG blend determined by 2D gradient map are, respectively, about 137.5 and 132.5 °C. The transition temperature of spin-coated films of P(HB-co-HHx)/PEG blends decreased as PEG composition of P(HB-co-HHx)/PEG blends increases. Furthermore, spin coated films of P(HB-co-HHx)/PEG blends show more transition temperature that have been interpreted in terms of different lamellar thicknesses in spin coated films.

Acknowledgments. This work was supported by the National Research Foundation of Korea (NRF) grants

funded by the Korea government (MEST) (No. 2009-0065428 and No. 2009-0087013) and the BK 21 program from the Ministry of Education, Science and Technology of Korea. The authors thank the Central Laboratory of Kangwon National University for the measurements of IRRAS spectra.

References

- Bastiolo, C. In *Handbook of Biodegradable Polymers*; Rapra Technology Limited; UK, 2005.
- Chiellini, E.; Solaro, R. In *Recent Advances in Biodegradable Polymers and Plastics*; Wiley-VCH; Weinheim, 2003.
- Satkowski, M. M.; Melik, D. H.; Autran, J.-P.; Green, P. R.; Noda, I.; Schechtman, L. A. In *Biopolymers*; Steinbüchel, A., Doi, Y., Eds.; Wiley-VCH: Weinheim, 2001; p 231.
- Noda, I.; Green, P. R.; Satkowski, M. M.; Schechtman, L. A. *Biomacromolecules* **2000**, *6*, 580.
- Sato, H.; Murakami, R.; Padermshoke, A.; Yamaguchi, H.; Terauchi, H.; Ekgasit, S.; Noda, I.; Ozaki, Y. *Macromolecules* **2004**, *37*, 3763.
- Furukawa, T.; Sato, H.; Murakami, R.; Zhang, J.; Duan, Y.-X.; Noda, I.; Ochiai, S.; Ozaki, Y. *Macromolecules* **2005**, *38*, 6445.
- Zhang, J.; Sato, H.; Furukawa, T.; Tsuji, H.; Noda, I.; Ozaki, Y. *J. Phys. Chem. B* **2006**, *110*, 24463.
- Sato, H.; Mori, K.; Murakami, R.; Ando, Y.; Takahashi, I.; Zhang, J.; Terauchi, H.; Hirose, F.; Senda, K.; Tashiro, K.; Noda, I.; Ozaki, Y. *Macromolecules* **2006**, *39*, 1525.
- Zhang, J.; Sato, H.; Noda, I.; Ozaki, Y. *Macromolecules* **2005**, *38*, 4274.
- Jung, Y. M.; Sato, H.; Noda, I. *Anal. Sci.* **2007**, *23*, 881.
- Furukawa, T.; Sato, H.; Murakami, R.; Zhang, J.; Noda, I.; Ochiai, S.; Ozaki, Y. *Polymer* **2007**, *48*, 1749.
- Vogel, C.; Wessel, E.; Siesler, H. W. *Biomacromolecules* **2008**, *9*, 523.
- Guo, L.; Sato, H.; Hashimoto, T.; Ozaki, Y. *Macromolecules* **2011**, *44*, 2229.
- Ji, H.; Kim, S. B.; Noda, I.; Jung, Y. M. *Spectrochimica Acta Part A* **2009**, *71*, 1873.
- Ji, H.; Hwang, H.; Kim, S. B.; Noda, I.; Jung, Y. M. *J. Mol. Struct.* **2008**, *883-884*, 167.
- Choi, H. C.; Ryu, S. R.; Ji, H.; Kim, S. B.; Noda, I.; Jung, Y. M. *J. Phys. Chem. B* **2011**, *114*, 10979.
- Noda, I.; Ozaki, Y. *Two-Dimensional Correlation Spectroscopy: Applications in Vibrational Spectroscopy*; John Wiley & Sons: Inc.; New York, 2004.
- Jung, Y. M.; Noda, I. *Appl. Spectrosc. Rev.* **2006**, *41*, 515.
- Noda, I. *Appl. Spectrosc.* **1993**, *47*, 1329.
- Jung, Y. M.; Shin, H. S.; Czarnik-Matusewicz, B.; Noda, I.; Kim, S. B. *Appl. Spectrosc.* **2002**, *56*, 1568.
- Chae, B.; Lee, S. W.; Jung, Y. M.; Ree, M.; Kim, S. B. *Appl. Spectrosc.* **2008**, *62*, 497.
- Jung, Y. M.; Shin, H. S.; Kim, S. B.; Noda, I. *J. Phys. Chem. B* **2008**, *112*, 3611.
- Avella, M.; Martescelli, E. *Polymer* **1988**, *29*, 1731.
- Izawa, K.; Ogasawara, T.; Masuda, H.; Okabayashi, H.; Noda, I. *Macromolecules* **2002**, *35*, 92.
- Lim, J. S.; Noda, I.; Im, S. S. *J. Polym. Sci. Part B: Polym. Phys.* **2006**, *44*, 2852.
- Czarnik-Matusewicz, B.; Kim, S. B.; Jung, Y. M. *J. Phys. Chem. B* **2009**, *113*, 559.
- Vogel, C.; Wessel, E.; Siesler, H. W. *Biomacromolecules* **2008**, *9*, 523.